Sensitivity to effective electroweak couplings in single top production at the LHC

D. Espriu*and J. Manzano†
Departament d'Estructura i Constituents de la Matèria and IFAE
Universitat de Barcelona, Diagonal, 647, E-08028 Barcelona

Abstract

We study the mechanism of single top production at the LHC in the framework of an effective electroweak lagrangian, analyzing the sensitivity of different observables to the magnitude of the effective couplings of the top. The analysis is carried out using the effective W approximation, whose validity in the present case is discussed. To be able to distinguish between left and right effective couplings one must necessarily measure the polarization of the top and this can only be achieved indirectly by measuring the angular distribution of top decay products. We show that a unique spin basis (in the top rest frame) exists that allows one to connect the top decay products angular distribution with the single top polarized production cross section.

UB-ECM-PF 99/20
March 2000

*espriu@greta.ecm.ub.es
†manzano@ecm.ub.es

1 Introduction

The standard model of electroweak and strong interactions has been, to this day, tested to a remarkable degree of accuracy, particularly in what concerns the neutral current sector. However it is clear that suffers from several theoretical drawbacks (naturalness, triviality,...) making it conceivable that it should be considered as an effective theory valid only at low energies ($\lesssim$ 1 TeV). Moreover since the Higgs particle has not been observed, with the current bound on the Standard Model Higgs at 106.2 GeV [1], it makes sense to consider as an alternative to the minimal Standard Model an effective theory without any physical light scalar fields and, in turn, containing an infinite set of effective operators, compatible with the electroweak and strong symmetries $SU(3)_c \times SU(2)_L \times U(1)_Y$, whose coefficients would parametrize physics beyond the Standard Model. The effective lagrangian is organized as an expansion in operators of increasing dimensionality normalized by some large mass. These higher dimensional operators are unimportant at low energies, but their effects can be felt when a new kinematic range, such as the one provided by LHC, becomes accessible. Within this framework [2] one can describe the low energy physics of theories exhibiting the pattern of symmetry breaking $SU(2)_L \times U(1)_Y \to U(1)_{em}$, in the understanding that this approach is useful as long as those particles not explicitly included in the effective lagrangian are much heavier than the scale of energies at which the effective lagrangian is to be used.

In this work we plan to investigate the new features that physics beyond the standard model, parametrized by an effective lagrangian of the type described, may introduce in the production of single top quarks through W-gluon fusion at the LHC. We will keep only the leading non-universal (i.e. not appearing in the standard model at tree level) effective operators in the low energy expansion. Namely, those operators of dimension four which were first classified by Appelquist et al. [3]. These operators are characteristic of strongly coupled theories and, strictly speaking, are absent in the minimal Standard Model and in modifications thereof containing only light fields. When particularizing to the W interactions, the net effect of these operators is to induce effective couplings of the gauge boson to the matter fields. Other possible effects from the dimension four operators are not physically observable in this process, as we shall see.

However, even in the minimal Standard Model, radiative corrections induce form factors in the vertices. Assuming a smooth dependence in the external momenta these form factors can be expanded in powers of momenta. At the lowest order in the derivative expansion the effect of radiative corrections can be encoded in effective couplings κ_L^{CC} and κ_R^{CC} in the charged sector and κ_L^{NC} and κ_R^{NC} in the neutral current sector (see e.g. [4]). Obviously these effective couplings take well defined, calculable values in the minimal Standard, and

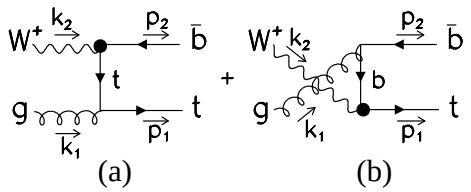

Figure 1: Feynman diagrams contributing to the single top production subprocess

any deviation from these values (which have not to our knowledge been yet determined in the Standard Model yet) would indicate the presence of new physics in the matter sector. To what extent can the LHC set direct bounds on these couplings, in particular in the third generation? Will the precision suffice to be sensitive to possible deviations with respect to the Standard Model? Will experiments be sensitive to electroweak radiative corrections?

At the LHC energy (14 TeV) the dominant mechanism of top production, with a cross section of 800 pb, is gluon-gluon fusion. This mechanism has nothing to do with the electroweak sector and thus is not the most adequate for our purposes (although is the one producing most of the tops and thus its consideration becomes necessary in order to study the top couplings through their decay, which will not be our main interest here).

At the tree level, electroweak physics enters the game in single top production. (For a recent review see e.g. [5].) At LHC energies the (by far) dominant electroweak subprocess contributing to single top production is given by a gluon (g) coming from one proton and a positively charged W^+ coming from the other (this process is also called t-channel production[6, 7]. This process is depicted in diagrams (a) and (b) of Fig.(1). The cross section for this process at the LHC is 250 pb, to be compared to 50 pb for the associated production with a W^+ boson and a b-quark extracted from the sea of the proton, and the 10 pb corresponding to quark-quark fusion (s-channel production). For a detailed discussion see [7]. For comparison, at the Tevatron (2 GeV) the cross section for W-gluon fusion is 2.5 pb, so the production of tops through this particular subprocess is copious at the LHC. Monte Carlo simulations including the analysis of the top decay products indicate that this process can be analyzed in detail at the LHC and traditionally has been regarded as the most important one for our purposes.

In a proton-proton collision a bottom-anti-top pair is also produced, through the subprocesses (a) and (b) of Fig.(2). However, these subprocesses are suppressed roughly by a factor of two (see Fig.(4)) because the proton has much lesser probability of emitting a W^- than emitting a W^+, and at any rate qualitative results are very similar to those corresponding to the subprocess of Fig.(1), from where the cross sections can be easily derived doing the appropriate changes.

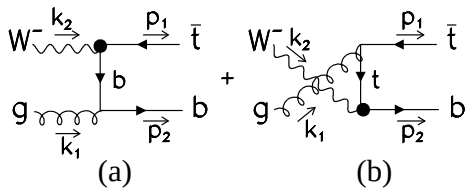

Figure 2: Feynman diagrams contributing to the single anti-top production subprocess

The contribution from operators of dimension five to top production via longitudinal vector boson fusion was estimated some time ago in [8], although the study was by no means complete. It should be mentioned that $t, \bar{t}$ pair production through this mechanism is very much masked by the dominant mechanism of gluon-gluon fusion, while single top production, through WZ fusion, is expected to be much suppressed compared to the mechanism presented in this paper, the reason being that both vertices are electroweak in the process discussed in [8], and that operators of dimension five are expected to be suppressed, at least at moderate energies, by some large mass scale. The contribution from dimension four operators as such has not, to our knowledge, been considered before, although the potential of single top production for measuring the CKM matrix element V_{tb}, and hence for setting bounds on κ_L^{CC}, has certainly been analyzed in the literature (see e.g. [7]). From these measurements bounds on the contribution from new physics to the coefficients of dimension four operators can be inferred.

In this paper the calculations are carried out in the framework of the so-called effective W approximation, that is the translation to the present case of the familiar Weizsäcker-William[9] approximation for photons, known to be accurate at high energies (see e.g. [10] for a discussion on errors and improvements) and very convenient. This approach is cacula-tionally simple and has all the attractive physical interpretation of the parton model. One certainly expects that the approximation, even for W's, is sufficiently good at LHC energies, where it has been amply used in the context of WW, WZ or $W\gamma$ scattering. (See e.g.[11] for a very recent application and references.) We shall later discuss in more detail to what extent these expectations are fulfilled.

In this work we have considered the production of polarized tops. As we shall see this is absolutely necessary if one wishes to set bounds on κ_R^{CC}, this effective coefficient being much smaller than κ_L^{CC} given that the latter is non-zero in the standard model at tree level. In doing so we have found results which are somewhat at variance with the recent work reported in [12]. It is not completely clear to us to what extent these discrepancies may be due to some of the approximations used or are genuine.

The paper is structured as follows. In section 2 we examine the dimension four operators

appearing in the effective lagrangian and verify that for this process the net effect of the eight independent operators can indeed be summarized in a couple of form factors. The effective W approximation is discussed and applied to the present problem in section 3. A general discussion of the results is presented in section 4. In section 5 we show the need to estimate the polarization of the top in order to extract the effective couplings. The proper way to estimate this polarization through the top decay products is analyzed in section 6. Finally the conclusions are collected in section 7. Technical details have been summarized in an Appendix.

2 Effective couplings and observables

The complete set of dimension four effective operators which may contribute to the top effective couplings is [3, 13]

$$\begin{aligned}
\mathcal{L}_4^1 &= i\delta_1 \bar{\mathrm{f}}\gamma^\mu U \left(D_\mu U\right)^\dagger L\mathrm{f}, \\
\mathcal{L}_4^2 &= i\delta_2 \bar{\mathrm{f}}\gamma^\mu U^\dagger \left(D_\mu U\right) R\mathrm{f}, \\
\mathcal{L}_4^3 &= i\delta_3 \bar{\mathrm{f}}\gamma^\mu \left(D_\mu U\right) \tau^3 U^\dagger L\mathrm{f} + h.c., \\
\mathcal{L}_4^4 &= i\delta_4 \bar{\mathrm{f}}\gamma^\mu U\tau^3 U^\dagger \left(D_\mu U\right) \tau^3 U^\dagger L\mathrm{f}, \\
\mathcal{L}_4^5 &= i\delta_5 \bar{\mathrm{f}}\gamma^\mu \tau^3 U^\dagger \left(D_\mu U\right) R\mathrm{f} + h.c., \\
\mathcal{L}_4^6 &= i\delta_6 \bar{\mathrm{f}}\gamma^\mu \tau^3 U^\dagger \left(D_\mu U\right) \tau^3 R\mathrm{f}, \\
\mathcal{L}_4^7 &= i\delta_7 \bar{\mathrm{f}}\gamma^\mu U\tau^3 U^\dagger D_\mu^L L\mathrm{f} + h.c., \\
\mathcal{L}_4' &= i\delta' \bar{\mathrm{f}}\gamma^\mu \tau^3 D_\mu^R R\mathrm{f} + h.c.,
\end{aligned} \tag{1}$$

where $L = \frac{1-\gamma^5}{2}$, $R = \frac{1+\gamma^5}{2}$ are the left and right projectors,

$$\begin{aligned}
D_\mu U &= \partial_\mu U + ig\frac{\tau}{2}\cdot\mathbf{W}_\mu U - ig'U\frac{\tau^3}{2}B_\mu, \\
D_\mu^L \mathrm{f} &= \left(\partial_\mu + ig\frac{\tau}{2}\cdot\mathbf{W}_\mu + ig'\frac{1}{6}B_\mu + ig_s\frac{\lambda}{2}\cdot\mathbf{G}_\mu\right)\mathrm{f}, \\
D_\mu^R \mathrm{f} &= \left(\partial_\mu + i\frac{g'}{2}\left(\tau^3 + \frac{1}{3}\right)B_\mu + ig_s\frac{\lambda}{2}\cdot\mathbf{G}_\mu\right)\mathrm{f},
\end{aligned} \tag{2}$$

and where f is a weak doublet of matter fields ((t,b) in our case). Generation mixing has been neglected. The above operators contribute to the different gauge boson-fermion-fermion vertices as indicated in table 1, where

$$\begin{aligned}
g_L &\equiv 1 + \delta g_L = 1 - \left(\delta_1 + \delta_4\right), \\
g_R &\equiv \delta g_R = \delta_2 - \delta_6,
\end{aligned} \tag{3}$$

Vertex	Feynman Rule
$\bar{t}gt$	$-ig_s\frac{\lambda}{2}^a\gamma_\mu\left(1+2\left(\delta_7 L+\delta' R\right)\right)$
$\bar{b}gb$	$-ig_s\frac{\lambda}{2}^a\gamma_\mu\left(1-2\left(\delta_7 L+\delta' R\right)\right)$
$\bar{t}W^+b$	$-\frac{i}{\sqrt{2}}g\gamma_\mu\left(g_L L+g_R R\right)$
$\bar{b}W^-t$	$-\frac{i}{\sqrt{2}}g\gamma_\mu\left(g_L^* L+g_R^* R\right)$

Table 1: Feynman rules for the vertices appearing in the subprocesses of Figs.(1) and (2).

These are the contributions from the matter sector of the effective electroweak lagrangian to the effective couplings κ_L^{CC} and κ_R^{CC}.

In addition, the operators $\mathcal{L}_4^7$ and $\mathcal{L}_4'$ also contribute to the quark self energies

$$\begin{aligned}\Sigma_u(p) &= -2\ \not{p}\left(\delta_7 L+\delta' R\right),\\ \Sigma_d(p) &= +2\ \not{p}\left(\delta_7 L+\delta' R\right),\end{aligned} \tag{4}$$

and to the counterterms required to guarantee the on-shell renormalization conditions [13]

$$\begin{aligned}&\delta Z_d^L=2\delta_7, && \delta Z_u^L=-2\delta_7,\\ &\delta Z_d^R=2\delta', && \delta Z_u^R=-2\delta',\\ &\delta m^d=-\left(\delta_7+\delta'\right)m^d, && \delta m^u=\left(\delta_7+\delta'\right)m^u,\end{aligned}$$

but when we take into account all these contributions, δ_7 and δ' vanish from the observables in the present case. It should be noted, however, that the internal quark line in the diagrams in Figs.(1) and (2) are never on-shell and the use of the equations of motion to eliminate, say $\mathcal{L}_4^7$, is a priori not justified. The net effect of the electroweak effective lagrangian in the charged current sector can thus be summarized, to the order we have considered, in the effective couplings g_L and g_R.

The effective couplings appropriate to the neutral sector

$$\begin{aligned}g_V^f &= I_f^3-2s_W^2Q_f+I_f^3\left(\delta_1-\delta_4-\delta_2-\delta_6\right)-\delta_3-\delta_5,\\ g_A^f &= I_f^3\left(1+\delta_1-\delta_4+\delta_2+\delta_6\right)-\delta_3+\delta_5,\end{aligned} \tag{5}$$

can be determined from the $Z\to f\bar{f}$ vertex [13], but at present not much is known from the $t\to b$ effective coupling. This is perhaps best evidenced by the fact that the current experimental results for the (left-handed) V_{tb} matrix element give [14]

$$\frac{|V_{tb}|^2}{|V_{td}|^2+|V_{ts}|^2+|V_{tb}|^2}=0.99\pm 0.29. \tag{6}$$

It should be emphasized that these are the 'measured' or 'effective' values of the CKM matrix elements, and that they do not necessarily correspond, even in the Standard Model, to the

entries of a unitary matrix on account of the presence of radiative corrections, even though these deviations with respect to unitary are expected to be small unless new physics is present. At the Tevatron the left-handed couplings are expected to be eventually measured with a 5% accuracy [15]

As far as experimental bounds for the right handed effective couplings is concerned, the more stringent ones come from the measurements on the $b \to s\gamma$ decay at CLEO [16]. Due to a m_t/m_b enhancement of the chirality flipping contribution, a particular combination of mixing angles and κ_R^{CC} can be bounded. The authors of [17] reach the conclusion that $|\mathrm{Re}(\kappa_R^{CC})| \leq 0.4 \times 10^{-2}$. However, considering κ_R^{CC} as a matrix in generation space, this bound only constraints the tb element. Other effective couplings involving the top remain virtually unrestricted from the data.

Certainly the previous bound on the right-handed coupling is a very stringent one. It is obvious that the LHC will never be able to compete with such a bound. Yet, the measurement will be a direct one, not through loop corrections. Equally important is that it will yield information on the ts and td elements too, by just replacing the quark exchanged in the t-channel in Fig.(1-b).

3 The effective W approximation

In order to calculate the cross section of the process $pp \to t\bar{b}X$ we have used the CTEQ4 structure functions [18] to determine the probability of extracting a parton with a given fraction of momenta from the proton. The u and d-type partons then radiate a W^+ or W^- boson, respectively.

In the effective W approximation these W bosons (both longitudinal and transverse) are treated as partons from the proton, carrying a fraction of the quark momentum and thus of the momentum of the proton. The W parton distribution function is, roughly speaking, the probability of producing a W with such a fraction of the momentum.

In the spirit of the Weiszäker-Williams approximation, to compute the cross-section for the process $pp \to t\bar{b}X$ (for instance) we write

$$\int_0^1 dy \int_0^1 d\hat{x} \int d^2k_T d^2k'_T |\mathcal{M}\left(pp \to W\left(k\right) g\left(k'\right)\right)|^2 \left(\frac{1}{k'^2}\right)^2 \left(\frac{1}{k^2 - M_W^2}\right)^2 |M\left(k, k'\right)|^2, \quad (7)$$

where $|M|^2$ is the physical squared amplitude for the subprocess $Wg \to t\bar{b}$ and $|\mathcal{M}|^2$ the analogous quantity for $pp \to gW$. In the subprocess, both the W and the gluon are assumed to be on-shell, i.e. is a physical, gauge independent, cross section. Of course the W is never on-shell. Kinematically, the W has a space-like four momentum, and it is off its mass shell by an amount which is, at least, M_W^2. However, at the energies which are characteristic

of the LHC, one expects the error to be small. The variables $\hat{x}$ and y are the fractions of the longitudinal proton momenta carried by the W and gluon, respectively. k_T and k'_T are the respective transverse momenta of W and gluon. If we place ourselves in the center-of-mass frame of the gluon and, say, the u parton, the W momentum can be written as $k = (\omega, k_T, xE)$, where $\omega = E - \sqrt{(1-x)^2E^2 + k_T^2}$. E is the energy of the u parton in that frame, and x the fraction of the parton momenta in the z direction, $xE = \hat{x}E_P$, E_P being the proton energy in the center-of-mass frame of the gluon and the u parton.

Using Eq.(7) we can write the cross section for the process in the form

$$\int_0^1 dy f_g(y) \int_0^1 d\hat{x} \int_{\hat{x}}^1 \frac{dx}{x} f_u(\frac{\hat{x}}{x}) f_W(x) \hat{\sigma}(\hat{x}p, yq) \tag{8}$$

The quantities $f_g(y)$ and $f_u(\frac{\hat{x}}{x})$ are the parton distribution functions of the gluon and u type parton. $\hat{\sigma}$ is the subprocess cross section. Equations 7 and 8 define the W parton distribution function $f_W(x)$. This was first calculated by Dawson[19] and by Kane, Repko and Rolnick[20]. There are, in fact, two parton distribution functions: one for transverse W's, $f_{W_T}(x)$, and another one for longitudinal ones, $f_{W_L}(x)$.

In Eq.(8) we have replaced the W and gluon momenta, k and k', by their z components $\hat{x}p$ and yq, respectively (p and q are the four-momenta of the protons.) The approximation thus involves neglecting the transverse momenta in $\hat{\sigma}$. Consequently the k^2 of the W, which is always spacelike is in practice approximated by $k^2 = 0$ in the prefactor and, furthermore, in $\hat{\sigma}$ one takes the physical value $k^2 = M_W^2$. As discussed above the effect of this last approximation will be small at high energies $E \gg M_W$.

In passing from Eq.(7) to Eq.(8) one averages over the possible values of the transverse momenta. For 'normal' partons (the gluon, for instance) this leads to a mass singularity as $k_T \to 0$; the distribution is clearly peaked at low values of k_T, leading to the familiar logarithmic dependence on the scale. On the other hand, for the W the integral over k_T is cut-off by M_W^2 and the mass singularity is absent. There is thus a natural spread in the distribution of k_T which makes the effective W approximation less accurate. Obviously the approximation becomes better the larger the value of E is. Dawson[19] and others [21] have estimated in some detail the accuracy of the approximation. Half the cross section for transverse W's comes from angles $\theta \leq \sqrt{M_W/2E}$ (in the center of mass frame of the u parton and the gluon), and the cross section is even more collimated for longitudinal W's. We have set a cut of 500 GeV in the sub-process invariant mass to guarantee the validity of the effective W approximation (that is, very low values of $\hat{x}$ are never considered).

The upper limit for the integral over k_T sets the scale normalizing the dependence on M_W of the structure functions. At the order we are working it is somewhat ambiguous to set a value for this scale. Some authors (see e.g. [11, 22]) take $k_T^{max} = E^2$ (E is the energy of the

u or the gluon in its center-of-mass frame). The kinematical upper limit for k_T^2 is actually $4E^2$ and this is the value that we have used in the present work. It should be borne in mind though that the uncertainty associated to using one value or another, while nominally subdominant is not so small at LHC energies, so the difference matters to some extent. At LHC energies using E^2 or $4E^2$ could easily lead to differences at the 20% level. With this proviso, the relevant expressions for f_{W_T} and f_{W_L} that we have used can be found in [20]. Next to leading calculations exist in the literature, but we do not feel that they are necessary for our purposes here[21].

The other approximation involved in using the effective W approximation is the neglection of the crossed interference term between longitudinal and transverse W's. The approximation is obviously correct if the process is clearly dominated either by longitudinal or by transverse W's. In the case of WW scattering[11] it is clear that the process is dominated by longitudinal W's (this is best seen by using the equivalence theorem[23]). In the case at hand, the cross sections of the elementary subprocesses of Fig.(1) are presented in the Appendix and it is not difficult to check that although longitudinal W's dominate (by roughly a factor of 3) they are of the same order. Fortunately it can be seen that integration over the azimutal angle makes the interference term to vanish[24, 21]. So in fact, the neglection of the interference term is not an approximation at all.

We have thus proceeded as follows. We have multiplied the parton distribution function of a gluon of a given momenta from the first proton by the sum of parton distribution functions for obtaining a u type quark from the second proton. Then we have multiplied this result by the probability of obtaining an on-shell transversal W^+ from those partons. We have repeated the process for a longitudinal vector boson. These results are then multiplied by the cross sections of the subprocesses of Fig.(1) corresponding to transversal or longitudinal W^+, respectively. At the end, these two partial results are added up to obtain the total $pp \to t\bar{b}X$ cross section.

Let us now discuss some of the approximations that we have *not* made. For instance, the bottom mass has been maintained all the way through. We have also worked with the exact polarization vectors for longitudinal W's

$$\varepsilon_L^\mu\left(k_2^\mu\right) = \frac{1}{M_W}\left(\left|\vec{k}_2\right|, k_2^0 \frac{\vec{k}_2}{\left|\vec{k}_2\right|}\right), \tag{9}$$

without making the approximation $\varepsilon_L^\mu \simeq k^\mu/M_W$ that is often made in this context.

Since typically, the top quark decays weakly well before strong interactions become relevant, we can in principle measure its polarization state with virtually no contamination of strong interactions (see e.g. [12] for discussions on how this could be done, but see also

our comments in section 6). In fact measuring the polarization turns out to be crucial if one wishes to analyze the left and right handed couplings separately. For this reason we have considered polarized cross sections for the subprocess and provided formulae for the production of polarized tops in a general reference frame (obviously within the context and limitations of the effective W approximation.) We have not made the approximation of replacing polarized top states by chirality states as this is a extremely poor one due to the large top mass, even at LHC energies. The top mass is taken to be 173 GeV throughout the paper.

4 A first look at the results

In this section we shall present the results of our analysis. To calculate the event production rate corresponding to different observables and compare them with the theoretical predictions we have used the integrating montecarlo program VEGAS [25]. We present results after one year run at full luminosity in one detector (100 fb^{-1} at LHC).

As previously stated, the total contribution to the electroweak vertices κ_L^{CC}, κ_R^{CC} has two sources: the effective operators parametrizing new physics, and the contribution from the universal radiative corrections. In the standard model, neglecting mixing, for example, we have a tree level contribution to the $\bar{t}W_\mu^+ b$ vertex given by $-\frac{i}{\sqrt{2}}\gamma_\mu gL$. Radiative corrections (universal and M_H dependent) modify the left effective coupling and generate a right handed one. These radiative corrections depend weakly on the energy of the process and thus in a first approximation we can take them as constant. Our purpose is to estimate the dependence of different LHC observables on these total effective couplings and how the experimental results can be used to set bounds on them. Assuming that the radiative corrections are known, this implies in turn a bound on the coefficients of the effective electroweak lagrangian.

Let us start by discussing the experimental cuts. We have, first of all, implemented a 500 GeV cut in the invariant mass of the subprocess. This is done in order to guarantee the validity of the effective W approximation. Due to geometrical detector constraints we adopt a pseudorapidity cut $|\eta| < 2.5$ both for the top and bottom. This corresponds to approximately 10 degrees. As for p_T we consider three different cuts: $|p_T| > 10$ GeV, $|p_T| > 20$ GeV and $|p_T| > 50$ GeV. Within the effective W approximation the W and gluon transverse momenta are neglected; this implies that the top and bottom p_T are identical.

In single top production a distinction is often made between $2 \to 2$ and $2 \to 3$ processes. The latter corresponds, in fact, to the process we have been discussing, the one represented in fig 1, in which a gluon from the sea splits into a $b\ \bar{b}$ pair. In the $2 \to 2$ process the b quark is assumed to be extracted from the sea of the proton. Of course the distinction between the two processes is merely kinematical and somewhat arbitrary. In the remains of the proton

(g_R, g_L)	N_-	N_+	$\frac{N_-}{N_+ + N_-}$
$(0.0, 1.0)$	$1.949(4) \times 10^5$	$1.229(4) \times 10^5$	.613
$(0.1, 1.0)$	$1.957(4) \times 10^5$	$1.245(4) \times 10^5$	.611
$(0.0, 1.1)$	$2.358(5) \times 10^5$	$1.487(4) \times 10^5$	.613

Table 2: Total number of events in single top production in the LAB helicity frame for different values of δg_L and δg_R. Values calculated with $p_T > 20$ GeV., $10^\circ < \theta < 170^\circ$ and $\sqrt{s} > 500$ GeV.

a $\bar{b}$ must be present, given that the proton has no net b content and thus the final state is also identical to the one we have been discussing. The figures for the cross sections presented in the introduction correspond to the kinematical cuts used in [7]. In the framework of our approximation all partons are deemed to have zero transverse momentum and hence the detection of a $\bar{b}$ in the fiducial zone, above the angular and/or p_T cuts, necessarily indicates that the $\bar{b}$ in the final state is 'hard'. A sufficiently generous cut in p_T ensures the validity of the approximation and the neglection of the $2 \to 2$ contributions.

As is implicit in the above discussion we do not advocate looking for processes with a single b in the fiducial region as a method of separating the signal (single top) from the background (mostly $t\bar{t}$) as proposed in [7]. First of all, looking for the signal in the low p_T region implies that the large QCD corrections, b parton distribution function etc. are to be trusted to a high degree of accuracy. In addition there is contamination from the Wt production mode. Finally, from an experimental viewpoint, it is always problematic to base a precision measurement in *not* having seen something. It is doubtful that the efficiency of the detector can be trusted to such a degree. For these reasons, the separation of the dominant (about three or four times bigger) $t\bar{t}$ mode should be done event by event based on the larger jet multiplicity of the latter, reconstruction of the top and antitop invariant mass and so on.

We shall start by considering the Standard Model tree-level predictions concerning single top production. In Table 1 we present our numerical results for production of polarized tops in the helicity basis in the LAB frame. The error quoted is the $\sqrt{N}$ statistical one. We have not included the errors associated to the approximations made in the effective W approximation, which we estimate to be at the 10% level. From this table we see that both polarizations appear roughly at a comparable rate, the number of negative helicity tops is just a mere 61%. This figure is in good agreement with the one reported in [12]

It may be interesting to compare these results with the ones we would obtain had we used chiral states, which have the advantage of being a Lorentz invariant concept. Of course there is no such thing as a massive chiral fermion. However one may think that at such energies the top mass is relatively unimportant. This is not so; the production is peaked in

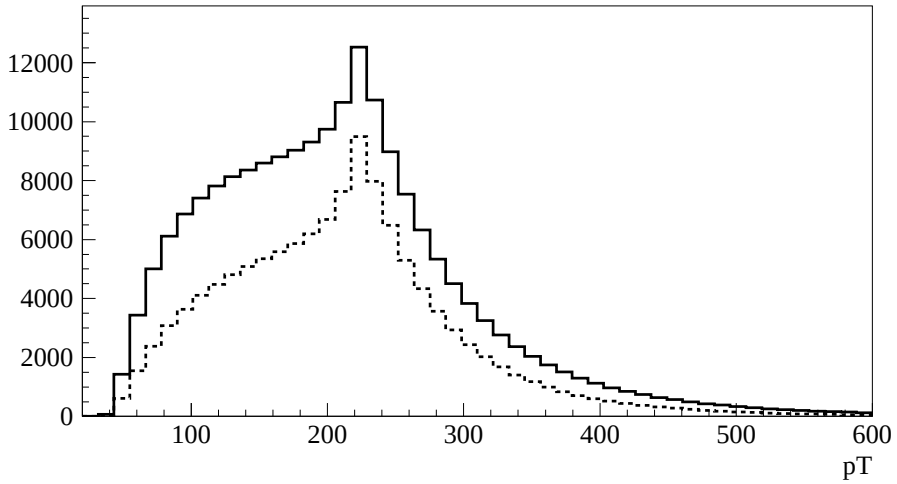

Figure 3: Expected number of (single) tops produced at the LHC vs. transversal momentum in the Standard Model. The solid (dotted) line corresponds to left (right) polarized top production. The subprocesses contributing to these histograms have been calculated at tree level in the electroweak theory. In the figure we show the results of the calculations for polarized top production in the LAB helicity basis. The histograms contain 50 bins in the range 20-600 GeV.

the 200 - 400 GeV region and the mass matters there. One can observe from the simulations that the production of left tops represents the 84% of the total single top production, this predominance of left tops in the tree level electroweak approximation is expected due to the suppression at high energies of right-handed tops because of the zero right coupling in the charged current sector. In fact the production of right-handed tops would be zero were it not for the chirality flip, due to the top mass, in the t-channel.

We have also calculated single anti-top production. In Fig.(4) we show two different histograms corresponding to the production of $\bar{t}$ with the two possible helicities in the LAB frame. All the histograms correspond to the tree level electroweak approximation and clearly show that single anti-top production is suppressed roughly by a factor of two with respect to single top production. This feature is general and is due to the different probability of extracting a W^- from a proton as compared to that of extracting a W^+. The relevant electroweak cross sections (see Appendix) are symmetric under the interchange of particle by antiparticle along with helicity flip.

It is interesting to note that the cross sections are dominated by transverse W's. This may sound a bit surprising at first since, as is well known, WW scattering is dominated by longitudinal W's. In fact as we have already pointed out the cross section for the elementary

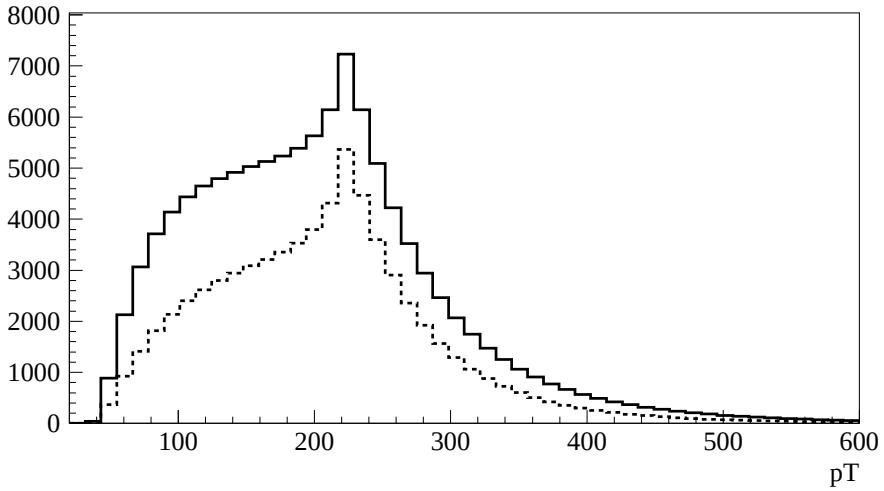

Figure 4: Expected number of (single) anti-top at the LHC vs. transversal momentum at tree level in the Standard Model. The solid (dotted) line corresponds to right (left) polarized anti-top production. All the histograms correspond to subprocesses calculated in the tree level electroweak approximation in the LAB helicity frame.The histograms contain 50 bins in the range 20-600 GeV.

subprocess is indeed larger for longitudinal W's, albeit not by a huge factor. It happens, however, that the probability of producing a transverse W is much larger and eventually these dominate.

In Figs. (5) and (6) we plot the angular distribution of the expected number of events in the (tree-level) Standard Model for negative and positive helicity tops in the LAB helicity frame, respectively. From the inspection of these figures two facts emerge: a) as expected the distribution is strongly peaked in the forward direction, with top and bottom produced back to back. b) The distribution is nevertheless flatter for right handed tops, showing more structure at large angles. In these figures a cut in $p_T > 20$ GeV has been implemented.

It is of some interest to repeat the analysis with the replacement $\varepsilon_L^\mu(k) \to k^\mu/M_W$ as is often done in the context of the equivalence theorem. The changes in the process mediated by longitudinal W's are minimal: less than a 5% .

Let us now depart from the tree-level Standard Model and consider non-zero values for δg_L and δg_R. Some numerical results are presented in table 2 for top production. The cuts are as the ones employed so far. Further insight can be obtained by plotting the expected number of events versus p_T and seeing how they compare to the Standard Model values. Some of results are presented in Figs. (7) and (8) for illustration. The results are somewhat disappointing in the sense that no spectacular distortions of the SM histograms are to be

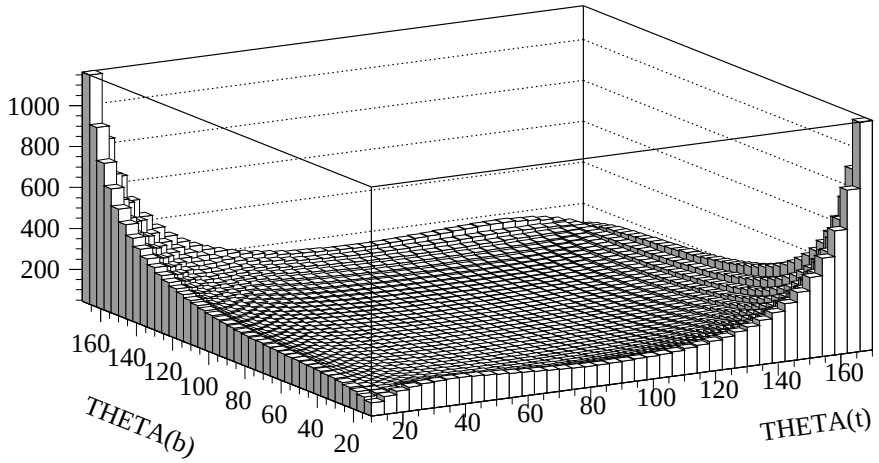

Figure 5: Expected angular distribution of single tops produced at the LHC in the Standard Model. Negative helicity states in the LAB helicity frame. Each bin in the histogram corresponds to 4×4 square degrees

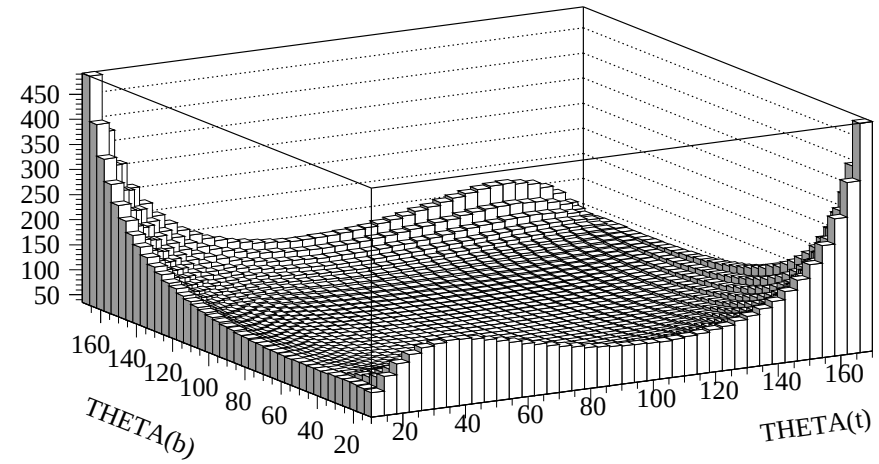

Figure 6: Expected angular distribution of single tops produced at the LHC in the Standard Model. Positive helicity states in the LAB helicity frame. Each bin in the histogram corresponds to 4×4 square degree

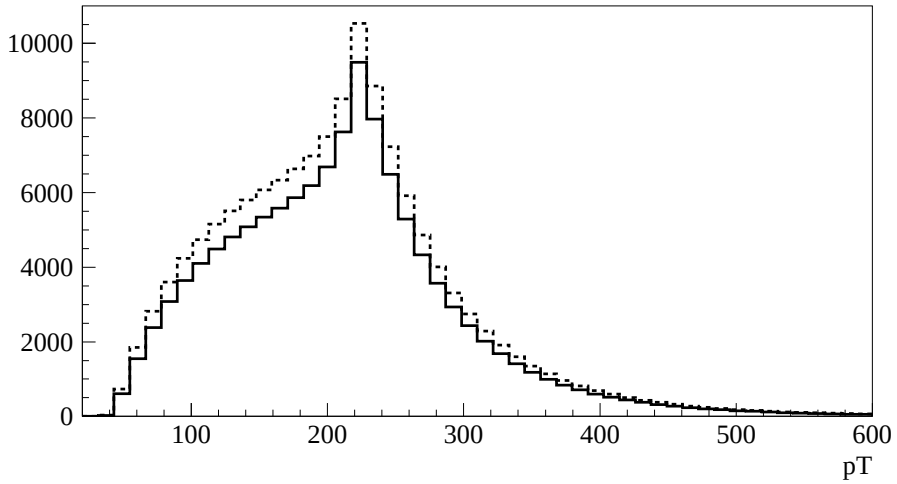

Figure 7: Comparison between the tree Standard Model prediction for the number of positively polarized tops (solid line) and those obtained with a value $g_R = 0.3$ for the effective right handed coupling (dotted line). The histograms contain 50 bins in the range 20-600 GeV.

seen when one switches on g_R. Indeed one obtains histogram profiles that are basically proportional to those of the tree-level Standard Model, both for positively and negatively polarized tops in the LAB helicity frame. Other frames show similar behaviour.

An estimate of the sensitivity to the effective couplings suggests that the combination $g_L^2 + g_R^2$, to which the total (unpolarized) cross section for top production is proportional can be determined with a precision ± 0.01. This is however a purely statical error and assumes that the absolute normalization is known, which is not true.

Still, a conclusion that can be drawn from these preliminary results is that the tops with positive helicity are more sensitive to the right handed coupling. This is not an unexpected result but it is not completely evident due to the large mass corrections for the top quark. However, it is clear that one has to work harder to extract, if at all, bounds on g_R. We postpone a more detailed analysis to the next section.

5 The differential cross section for polarized tops

Using general symmetry arguments, it is not difficult to convince oneself that the squared amplitude for the $gW^+ \to t\bar{b}$ subprocess, with a top positively polarized in the $\hat{n}$ direction, can be written at tree level as (see Appendix for notation)

$$|M|^2_{\hat{n}} = \left(|g_R|^2 + |g_L|^2\right) a + \left(|g_R|^2 - |g_L|^2\right) b_n + m_b m_t \frac{g_R^* g_L + g_L^* g_R}{2} c \qquad (10)$$

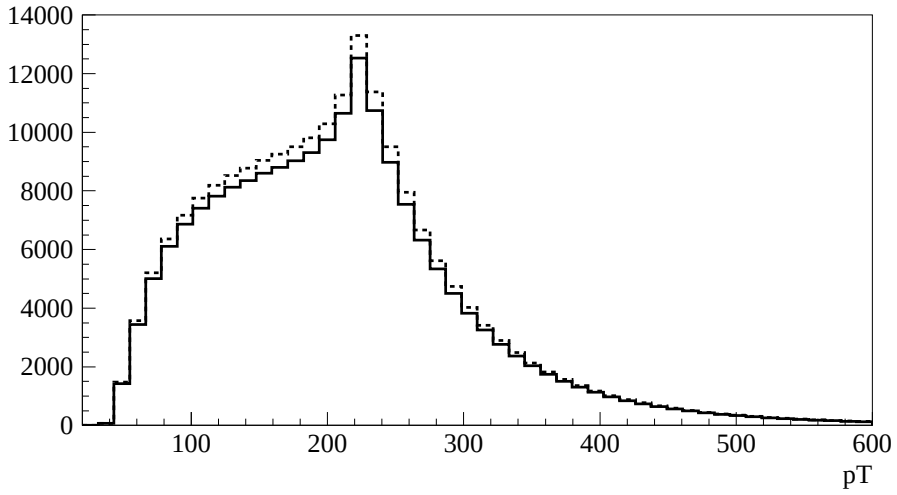

Figure 8: Same as in the previous figure, but for negatively polarized tops in the LAB helicity frame (solid line for SM).The histograms contain 50 bins in the range 20-600 GeV.

$$= \left(\begin{array}{cc} g_R^* & g_L^* \end{array} \right) \left(\begin{array}{cc} a+b_n & \frac{m_b m_t}{2} c \\ \frac{m_b m_t}{2} c & a-b_n \end{array} \right) \left(\begin{array}{c} g_R \\ g_L \end{array} \right) \tag{11}$$

$$\equiv \left(\begin{array}{cc} g_R^* & g_L^* \end{array} \right) A \left(\begin{array}{c} g_R \\ g_L \end{array} \right), \tag{12}$$

where a, b_n, and c are independent of the effective couplings g_R and g_L and b_n is the only piece that depends on the top spin four-vector n. In fact, b_n changes sign when the spin of the top is reversed. From Eq.(12) we also observe that possible CP violating phases in the coupling appear suppressed by the bottom mass and involve both g_L and g_R.

The analytical form of the coefficients a, b_n and c can be deduced from the formulae given in the Appendix. To obtain the squared amplitude of the whole process $pp \to t\bar{b}X$ we have to multiply those expressions by the corresponding W and gluon parton distribution functions and make the sums over parton species and polarizations. All these operations respect the general form given in Eq.(12) for each kinematical configuration individually. Finally, to obtain the total cross section we have to integrate over all possible final kinematical configurations. We shall denote by $\sigma_{\hat{n}}$ the total cross section for producing a polarized top with its spin pointing in the $\hat{n}$ direction. The decomposition of $\sigma_{\hat{n}}$ is similar to that of $|M|^2_{\hat{n}}$, but replacing a, b_n and c by $\bar{a}$, $\bar{b}_n$ and $\bar{c}$ in the expression for the total cross section. The quantities $\bar{a}$, $\bar{b}_n$ and $\bar{c}$ are given in tables 3 and 4.

The number of positively and negatively polarized tops (antitops) in a given spin direction in a particular reference frame will be given by (recall that polarization is not a Lorentz

cut	$\bar{a}$	$\bar{b}_n$	$m_b m_t \bar{c}$
$p_T > 10$ GeV	158960	35991	-3739
$p_T > 20$ GeV	158897	35997	-3738
$p_T > 50$ GeV.	158405	35726	-3735

Table 3: values of $\bar{a}$, $\bar{b}_n$ and $m_b m_t \bar{c}$ for top production in the LAB helicity frame with three different cuts in p_T .

cut	$\bar{a}$	$\bar{b}_n$	$m_b m_t \bar{c}$
$p_T > 10$ GeV	90117	-21263	-1995
$p_T > 20$ GeV	90122	-21268	-1994
$pT > 50$ GeV	89819	-21127	-1991

Table 4: values of $\bar{a}$, $\bar{b}_n$ and $m_b m_t \bar{c}$ for anti-top production in the LAB helicity frame with three different cuts in p_T.

invariant concept)

$$\begin{aligned} N_+ &= \left(|g_R|^2 + |g_L|^2\right)\bar{a} + \left(|g_R|^2 - |g_L|^2\right)\bar{b}_n + m_b m_t \frac{g_R^* g_L + g_L^* g_R}{2}\bar{c}, \\ N_- &= \left(|g_R|^2 + |g_L|^2\right)\bar{a} - \left(|g_R|^2 - |g_L|^2\right)\bar{b}_n + m_b m_t \frac{g_R^* g_L + g_L^* g_R}{2}\bar{c}, \end{aligned} \tag{13}$$

where $\bar{a}$, $\bar{b}_n$ and $m_b m_t \bar{c}$ are given in tables 3 and 4 for the LAB helicity frame. As we can see the numbers are only mildly dependent on the actual value of p_T^{cut} (but remember that the cut in pseudorapidity equivalent to 10 degrees is the same in all three cases).

If we neglect the term proportional to m_b, which is always at least an order of magnitude smaller that the other two, we see that $(N_+ - N_-)/(N_+ + N_-)$ is proportional to $g_L^2 - g_R^2$. On the other hand, the total number of tops (antitops) is proportional to $g_L^2 + g_R^2$. Although the above numbers refer to the total cross section, this remains valid for any given momenta in the final state; i.e. for any kinematical configuration. Consequently, it is not possible to separate g_R from g_L unless the top polarization is determined.

Returning to the discussion of the general aspects of Eq.(12) we observe that A is a symmetric matrix and then it is diagonalizable. Moreover, from the positivity of $|M|^2_{\hat{n}}$ we immediately arrive at the constraints

$$\det A = a^2 - b_n^2 - \frac{m_b^2 m_t^2 c^2}{4} \geq 0, \tag{14}$$

$$\frac{1}{2}\mathrm{Tr}A = a \geq 0. \tag{15}$$

In order to have a 100% polarized top we need two conditions to be verified. First of all, there must exist a spin four-vector n that saturates the constraint (14) for each kinematical

situation, that is we need A to have a zero eigenvalue. In general such n need not exist and, should it exist, is in any case independent of the anomalous couplings g_R and g_L. Moreover, provided this n exists, the couplings g_L, g_R must be a solution to the equation $|M|^2_{\hat{n}} = 0$, or, equivalently, to the eigenvector equation

$$A \begin{pmatrix} g_R \\ g_L \end{pmatrix} = 0, \tag{16}$$

i.e. they must correspond to the zero eigenmode of A. To illustrate these considerations let us give an example: In the unphysical situation where $m_t \to 0$ it can be shown that there exists two solutions to the saturated constraint (14), namely

$$m_t n^\mu \to \pm \left(|\vec{p}_1| \, , p_1^0 \frac{\vec{p}_1}{|\vec{p}_1|} \right), \tag{17}$$

once we have found this result we plug it in the expression (16) and we find the solutions $(0, g_L)$ with g_L arbitrary for the positive sign in (17) and $(g_R, 0)$ with g_R arbitrary for the negative sign. That is, physically we have zero probability of producing a right handed top when we have only a left handed coupling and viceversa when we have only a right handed coupling. Note that if our theory had a massless top and any other values for the couplings g_R and g_L then there would be no direction of 100% polarization.

This can be understood by remembering that the spin of the top particle is in general entangled with the other particles in the final state and since we are tracing over the unknown spin degrees of freedom of of those particles we do not expect in general to end up with a top in a pure polarized state, although this is not impossible as it is shown by the above example. In the physical situation where $m_t \neq 0$ we have checked numerically in a large amount of randomly chosen positions in phase space that the constraint (14) is never saturated (the reason apparently being that the tranverse and longitudinal W subprocess cross section have different signs for their b_n parts). Thus, we conclude that in general the top particle is produced in a mixed state without any defined direction of polarization. This fact by no means rules out the possibility of finding a spin frame where, if not a 100%, a high level of polarization can be achieved. In our case we have not succeded in finding a physically meaningful frame where the degree of polarization is larger than 70% . In view of this we have opted to present our results in the LAB helicity frame. These conclusions are somewhat at variance with the results recently presented in [12], where a frame is suggested with a degree of polarization around 90% . It is not clear to us whether this discrepancy is due to the approximations involved in the effective W treatment. For instance some of the reference frames suggested in [12] cannot be really exactly implemented in our case, although we would have expected a smaller discrepancy. On the other hand the authors of [12] have neglected

the b mass, although again one would not expect this to make a big difference. The issue certainly needs further clarification.

6 Measuring the top polarization from its decay products

As we just discussed, it is not possible to distinguish left from right couplings unless the polarization of the top is determined. The polarization can only be determined through the decay products of the top. The cleanest way is provided by the charged lepton resulting from the decay

$$t \to b\left(W^+ \to l^+\nu_l\right), \tag{18}$$

In the Standard Model (at tree level) given a top polarized in the $\hat{n}$ direction in its rest frame, the lepton l^+ produced in the decay of the top via the above process has an angular distribution [26]

$$\frac{d\sigma}{d(\cos\theta)} \sim 1 + \cos\theta, \tag{19}$$

θ is the axial angle, measured from the direction of $\hat{n}$, formed by the momentum of the outgoing lepton and $\hat{n}$.

What can we do when the top is in a mixed state with no 100% polarization in any direction? The first naive answer would be: Let $\hat{n}$ be any axis in the top rest frame. If we measure the spin of the top we will have a probability p_+ (with $0 \leq p_+ \leq 1$) of finding it pointing in that given direction and a probability $p_- = 1 - p_+$ in the opposite direction so the angular distribution for the lepton would be

$$\frac{d\sigma}{d(\cos\theta)} \sim p_+\left(1+\cos\theta\right) + p_-\left(1-\cos\theta\right) \tag{20}$$

$$= 1 + \left(p_+ - p_-\right)\cos\theta. \tag{21}$$

The problem with formula (21) is that the angular distribution for the lepton depends on the arbitrary chosen axis $\hat{n}$ and this cannot be correct. The right answer can be obtained by noting the following facts

- Given a vector $\hat{n}$ in the rest frame and the spin basis associated to it $\{|+\hat{n}\rangle, |-\hat{n}\rangle\}$ the top spin state in described by a 2×2 density matrix ρ

$$\rho = \rho_+ |+\hat{n}\rangle\langle+\hat{n}| + \rho_- |-\hat{n}\rangle\langle-\hat{n}| + b\,|+\hat{n}\rangle\langle-\hat{n}| + b^*\,|-\hat{n}\rangle\langle+\hat{n}|, \tag{22}$$

  which is in general not diagonal ($b \neq 0$) and whose coefficients depend on the rest of kinematical variables determining the differential cross section.

- From the calculation of the polarized cross section we only determine the diagonal elements $\rho_\pm = p_\pm = \sigma_{\pm\hat{n}}/\left(\sigma_{+\hat{n}} + \sigma_{-\hat{n}}\right)$.

- Given ρ in any orthogonal basis determined (up to phases) by $\hat{n}$ we can change to another basis that diagonalizes ρ. Since the top is a spin 1/2 particle, this basis will correspond to a given vector $\hat{n}_d$.

- Once we have ρ is written in a diagonal form then Eq.(21) is trivially correct with $p_\pm = \rho_\pm$ and now θ is unambiguously measured from the direction of $\hat{n}_d$.

From the above the first question that comes to our minds is if there exists a way to determine $\hat{n}_d$ without knowing the off-diagonal matrix elements of ρ. The answer is yes. It is an easy exercise of elementary quantum mechanics that given a 2×2 hermitian matrix ρ the eigenvector with largest (lowest) eigenvalue correspond to the unitary vector that maximizes (minimizes) the bilinear form $\langle v| \rho |v\rangle$ constrained to $\langle v|v\rangle = 1$. Since an arbitrary normalized $|v\rangle$ can be written (up to phases) as $|+\hat{n}\rangle$ and in that case $\rho_+ = p_+$ then the correct $\hat{n}_d$ entering in Eq.(21) for a given kinematical configuration is the one that maximizes the differential cross section for that specific set of momenta.

What happens when we move away from the Standard Model? The above analysis remains essentially the same also for $g_R \neq 0$, except that now the formula to use for the angular distribution of the lepton produced in the decay of the top is[26]

$$\frac{d\sigma}{d(\cos\theta)} \sim 1 + (p_+ - p_-)\left(1 - \frac{1}{4}\left|g_R\right|^2 h\right)\cos\theta. \tag{23}$$

where $h \simeq 0.57$ [26]. Formula (23) deserves some comments

- First of all we remember that θ is the angle (in the top rest frame) between the $\hat{n}$ that maximizes the difference $p_+ - p_-$ and the three momentum of the lepton.

- Taking into account the above comment and that $p_+ - p_-$ depends on $|g_L|^2$ and $|g_R|^2$ (we have neglected m_b and therefore the dependence on $g_R^* g_L + g_L^* g_R$), we have also that the direction where the lepton has maximum probability of being emitted depends on the value of the effective couplings.

- From the computational point of view, formula (23) is not an explicit formula because involves a process of maximization for each kinematical configuration.

- Usually [12] formula (23) is presented for an arbitrary choice of the spin base $\{|\pm\hat{n}\rangle\}$ in the top rest frame. This is incorrect because it does not take into account that, in general, the top spin density matrix is not diagonal in that basis.

7 Conclusions

We have analyzed the observable effects of the operators of dimension four in the most general effective lagrangian describing the matter sector of the Standard Model in single top production. At the order we are computing all effects can be summarized into effective left and right couplings.

We have done a complete calculation of the subprocess cross sections for the production of single (polarized) tops or anti-tops including all mass corrections and without using the equivalence theorem in an arbitrary frame. We have then used the effective W approximation in order to calculate the probability of obtaining a W boson from a proton with a given fraction of the proton longitudinal momentum and convoluted this probability, along with the equivalent one for the gluon, with the subprocess cross section, à la Weiszäcker and Williams. The approximation implies neglecting the transversal motion in the initial state. To ensure the validity of the approximation at LHC energies we have put a lower cut-off of 500 GeV in the invariant mass of the subprocess.

The cross section has been computed using a variety of cuts in angles and p_T. We have studied the angular and transversal momentum distribution of the top and (anti)bottom produced. The calculations have been performed both in the (tree level) Standard Model and with arbitrary couplings g_L, g_R, in particular with a view to directly determine or bound g_R from single top or antitop production. We provide formulae for the total cross section for arbitrary values of g_L and g_R. The unpolarized cross section is only sensitive to the combination $g_L^2 + g_R^2$. To disentangle the left and right couplings a measurement of the spin of the top is required.

We have discussed in detail under which circumstances the top are expected to be polarized and seen that this is not the case for arbitrary couplings. The top state is described by a spin density matrix. From that density matrix a unique basis emerges where a correlation can be established between the direction of the lepton in which the top decays and the spin of the top. This basis depends on the kinematical configuration and it must be re-determined for any event. The correlation thus involves g_L and g_R in a complicated non-linear way, but a theoretically clean distribution can then be obtained for any value of the effective couplings and compared to the experimental data.

8 Acknowledgments

We would like to thank A.Dobado, M.J.Herrero, J.R.Peláez and E.Ruíz-Morales for discussions, and R.Miquel for several remarks concerning the experimental feasibility of the analysis. We would also like to thank W.Hollik for encouraging us to present preliminary

results in the LHC CERN Workshop. J.M. acknowledges a fellowship from Generalitat de Catalunya, grant 1998FI-00614. Financial support from grants AEN98-0431, 1998SGR 00026 and EURODAPHNE is greatly appreciated.

A Subprocesses cross sections

In order to write the cross section of the subprocess, we define the spin four-vector corresponding to having the spin pointing in the $\hat{n}$ direction as

$$n^{\mu} \equiv \frac{1}{\sqrt{\left(p_1^0\right)^2 - \left(\vec{p}_1 \cdot \hat{n}\right)^2}} \left(\vec{p}_1 \cdot \hat{n}, p_1^0 \hat{n}\right), \tag{24}$$

with the properties

$$n^2 = -1, \qquad n \cdot p_1 = 0, \tag{25}$$

which reduces in the case of helicity ($\hat{n} = \pm \frac{\vec{p}_1}{|\vec{p}_1|}$) to

$$n^{\mu} \equiv \pm \frac{1}{m_t} \left(\left|\vec{p}_1\right|, p_1^0 \frac{\vec{p}_1}{|\vec{p}_1|} \right). \tag{26}$$

Thee differential cross section of the $gW \to t\bar{b}$ subprocess is

$$d\sigma = \frac{1}{32\pi} \frac{|p'|}{p E_{cm}^2} |M|^2 \, d\left(\cos\theta\right), \tag{27}$$

where we have written the expression in the subprocess center of mass frame. In this frame

$$\begin{aligned}
k_1 &= \left(\begin{array}{cccc} E_1 & 0 & 0 & p \end{array} \right) = \left(\begin{array}{cccc} p & 0 & 0 & p \end{array} \right), \\
k_2 &= \left(\begin{array}{cccc} E_2 & 0 & 0 & -p \end{array} \right) = \left(\begin{array}{cccc} \sqrt{M_W^2 + p^2} & 0 & 0 & -p \end{array} \right), \\
p_1 &= \left(\begin{array}{cccc} E_1' & p' \sin\theta & 0 & p' \cos\theta \end{array} \right), \\
p_2 &= \left(\begin{array}{cccc} E_2' & -p' \sin\theta & 0 & -p' \cos\theta \end{array} \right), \\
E_{cm} &= E_1 + E_2, \\
p' &= \sqrt{\left(\frac{E_{cm}^2 + m_b^2 - m_t^2}{2E_{cm}} \right)^2 - m_b^2},
\end{aligned} \tag{28}$$

and

$$|M|^2 = g_s^2 O_{ij} A_{ij} = g_s^2 \left(O_{11} A_{11} + O_{22} A_{22} + O_c \left(A_{12} + A_{21} \right) \right), \tag{29}$$

with

$$\begin{aligned}
O_{11} &= \frac{1}{4\left(k_1 \cdot p_1\right)^2}, \\
O_{22} &= \frac{1}{4\left(k_1 \cdot p_2\right)^2}, \\
O_c &= O_{12} = O_{21} = \frac{1}{4\left(k_1 \cdot p_1\right)\left(k_1 \cdot p_2\right)}.
\end{aligned} \tag{30}$$

After averaging over gluon colours and transverse polarizations, and summing over fermion colours we have

$$\begin{aligned} A_{11} &= A_{11}^{(+)} + A_{11}^{(-)} + m_t m_b \frac{g_R^* g_L + g_L^* g_R}{2} \varepsilon^2 \left\{ m_t^2 - k_1 \cdot p_1 \right\} \\ &\quad + m_t^2 \left(|g_L|^2 + |g_R|^2 \right) \left\{ 2 \left(\varepsilon \cdot p_2 \right) \left(\varepsilon \cdot (k_1 - p_1) \right) - \varepsilon^2 \left(p_2 \cdot (k_1 - p_1) \right) \right\}, \end{aligned} \tag{31}$$

with

$$\begin{aligned} A_{11}^{(\pm)} &\equiv |g_\pm|^2 \, \varepsilon \cdot p_2 \left\{ 2 \left((k_1 - p_1) \cdot \varepsilon \right) \left((k_1 - p_1) \cdot \frac{p_1 \pm m_t n}{2} \right) - (k_1 - p_1)^2 \left(\varepsilon \cdot \frac{p_1 \pm m_t n}{2} \right) \right\} \\ &\quad - |g_\pm|^2 \frac{\varepsilon^2}{2} \left\{ 2 \left((k_1 - p_1) \cdot p_2 \right) \left((k_1 - p_1) \cdot \frac{p_1 \pm m_t n}{2} \right) - (k_1 - p_1)^2 \left(p_2 \cdot \frac{p_1 \pm m_t n}{2} \right) \right\} \\ &\quad + |g_\pm|^2 \frac{m_t^2}{2} \left\{ 2 \left(\varepsilon \cdot p_2 \right) \left(\varepsilon \cdot \frac{p_1 \mp m_t n}{2} \right) - \varepsilon^2 \left(p_2 \cdot \frac{p_1 \mp m_t n}{2} \right) \right\}, \end{aligned} \tag{32}$$

and

$$A_{22} = A_{22}^{(+)} + A_{22}^{(-)} + m_b m_t \frac{g_R^* g_L + g_L^* g_R}{2} \left\{ p_2 \cdot \varepsilon^2 \left(p_2 - k_1 \right) \right\}, \tag{33}$$

with

$$\begin{aligned} A_{22}^{(\pm)} &\equiv |g_\pm|^2 \, p_2 \cdot (k_2 - p_1) \left\{ 2 \left(\varepsilon \cdot (k_2 - p_1) \right) \left(\varepsilon \cdot \frac{p_1 \pm m_t n}{2} \right) - \varepsilon^2 \left((k_2 - p_1) \cdot \frac{p_1 \pm m_t n}{2} \right) \right\} \\ &\quad - \frac{|g_\pm|^2}{2} (k_2 - p_1)^2 \left\{ 2 \left(\varepsilon \cdot p_2 \right) \left(\varepsilon \cdot \frac{p_1 \pm m_t n}{2} \right) - \varepsilon^2 \left(p_2 \cdot \frac{p_1 \pm m_t n}{2} \right) \right\} \\ &\quad + m_b^2 \frac{|g_\pm|^2}{2} \left\{ 2 \left(\varepsilon \cdot (4k_1 - 3p_2) \right) \left(\varepsilon \cdot \frac{p_1 \pm m_t n}{2} \right) - \varepsilon^2 \left((4k_1 - 3p_2) \cdot \frac{p_1 \pm m_t n}{2} \right) \right\}, \end{aligned} \tag{34}$$

and

$$\begin{aligned} A_{12} + A_{21} &= A_c^{(+)} + A_c^{(-)} \\ &\quad - m_b m_t \frac{g_R^* g_L + g_L^* g_R}{2} \left\{ \varepsilon^2 \left[2 \left(p_2 \cdot p_1 \right) - \left((p_2 + p_1) \cdot k_1 \right) \right] + 2 \left(\varepsilon \cdot k_1 \right)^2 \right\} \\ &\quad + \frac{|g_R|^2 + |g_L|^2}{2} \left\{ 2 m_t^2 \left(\varepsilon \cdot p_2 \right) \left(\varepsilon \cdot (k_2 - p_1) \right) - m_b^2 m_t^2 \varepsilon^2 \right\}, \end{aligned} \tag{35}$$

with

$$\begin{aligned} A_c^{(\pm)} &= 2 \left| g_\pm \right|^2 \left(\varepsilon \cdot p_2 \right) \left\{ \left((k_1 - p_1) \cdot \frac{p_1 \pm m_t n}{2} \right) \left(\varepsilon \cdot (k_2 - p_1) \right) \right. \\ &\quad \left. - \left(\frac{p_1 \pm m_t n}{2} \cdot (k_2 - p_1) \right) \left(k_1 \cdot \varepsilon \right) \right\} \\ &\quad - 2 \left| g_\pm \right|^2 \left(\varepsilon \cdot \frac{p_1 \pm m_t n}{2} \right) \left\{ \left(\varepsilon \cdot p_2 \right) \left(p_1 \cdot (k_1 - p_2) \right) \right. \\ &\quad + \left(\varepsilon \cdot (k_2 - p_1) \right) \left((k_1 - p_1) \cdot p_2 \right) \\ &\quad \left. - \left(\varepsilon \cdot (k_1 - p_1) \right) \left(p_2 \cdot (k_2 - p_1) \right) \right\} \end{aligned}$$

$$
\begin{aligned}
&+ |g_\pm|^2 \varepsilon^2 \left\{ (p_2 \cdot (k_1 - p_1)) \left((k_2 - p_1) \cdot \frac{p_1 \pm m_t n}{2} \right) \right. \\
&+ \left(p_2 \cdot \frac{p_1 \pm m_t n}{2} \right) ((k_2 - p_1) \cdot (k_1 - p_1)) \\
&\left. - (p_2 \cdot (k_2 - p_1)) \left((k_1 - p_1) \cdot \frac{p_1 \pm m_t n}{2} \right) \right\} \\
&-2 |g_\pm|^2 m_b^2 (\varepsilon \cdot (k_1 - p_1)) \left(\varepsilon \cdot \frac{p_1 \pm m_t n}{2} \right), \qquad (36)
\end{aligned}
$$

In the above expressions, ε is the polarization of the W^+ boson and in order to shorten the formulae we use the notation $g_+ \equiv g_R, g_- \equiv g_L$.

For the subprocess of Fig.(2) we have to perform the following changes in the expressions for the single top production.

$$
\begin{aligned}
\varepsilon &\leftrightarrow \varepsilon^*, \\
n &\leftrightarrow -n, \\
p_2 &\leftrightarrow -p_2, \\
p_1 &\leftrightarrow -p_1, \\
k_2 &\leftrightarrow -k_2, \\
k_1 &\leftrightarrow -k_1, \qquad (37)
\end{aligned}
$$

but since we can take the W boson polarization real and the cross section is even under the above sign changes, the subprocess cross section is exactly the same for single top or anti-top production.

References

[1] J.Marco, for the DELPHI collaboration, talk at the LEP Committee meeting, November 1999.

[2] T.Appelquist and C.Bernard, Phys. Rev. D22 (1980) 200; A.Longhitano, Phys. Rev. D22 (1980) 1166; A. Longhitano, Nucl. Phys. B188 (1981) 118; R.Renken and M.Peskin, Nucl. Phys. B211 (1983) 93; A.Dobado, D.Espriu and M.J.Herrero, Phys. Lett. B255 (1991) 405.

[3] T.Appelquist, M.Bowick, E.Cohler and A.Hauser, Phys. Rev. D31 (1985) 1676.

[4] C.P.Burgess, S.Godfrey, H.Konig, D.London and I.Maksymyk, Phys. Rev. D 49 (1994) 6115; E.Malkawi and C.P.Yuan, Phys. Rev. D50 (1994) 4462, Phys. Rev. D52 (1995) 472.

[5] T.M.P. Tait, Ph.D. Thesis, Michigan State University, 1999, hep-ph/9907462.

[6] S.Dawson, Nucl. Phys. B249 (1985) 42; S.Willenbrock and D.Dicus, Phys. Rev. D34 (1986) 155; C.P.Yuan, Phys. Rev. D41 (1990) 42; R.K.Ellis and S.Parke, Phys. Rev. D46 (1992) 3785; G.Bordes and B. van Eijk, Z. Phys. C 57 (1993) 81, Nucl. Phys. B435 (1995) 23; D.O.Carlson, Ph.D. Thesis, Michigan State University, 1995, hep-ph/9508278; T.Stelzer, Z.Sullivan and S.Willenbrock, Phys. Rev. D56 (1997) 5919.

[7] T.Stelzer, Z.Sullivan and S.Willenbrock,Phys. Rev. D58 (1998) 094021.

[8] F.Larios and C.P.Yuan, Phys. Rev. D55 (1997) 7218.

[9] C.Weiszäcker and E.Williams, Z. Phys. 88 (1934) 244.

[10] S.Frixione, M.Mangano, P.Nason and G.Ridolfi, Phys. Lett. B319 (1993) 339.

[11] A. Dobado, M. J. Herrero, J. R. Pelaez, and E. Ruiz Morales, hep-ph/9912224

[12] S.Parke, *Proceedings of the International Symposium on Large QCD Corrections and New Physics*, Hiroshima, 1997, Fermilab-Conf-97-431-T, hep-ph/9712512; G.Mahlon and S.Parke, Fermilab-Pub-99/361-T, hep-ph/9912458.

[13] E.Bagan, D.Espriu, J.Manzano, Phys. Rev. D60, (1999) 114035.

[14] C.Caso et al (The Particle Data Group), European Phys. J. C3 (1998) 1.

[15] D.Amidei and C.Brock, *Report of the the TeV2000 study group on future electroweak physics at the Tevatron*, FERMILAB-PUB-96-082, 1996.

[16] T.Swarnicki (for the CLEO collaboration), *Proceedings of the 1998 International Conference on HEP*, vol. 2, 1057.

[17] F.Larios, M.A.Perez and C.P.Yuan, hep-ph/9903394; F.Larios, E.Malkawi, C.P.Yuan, Acta Phys. Polon. B27 (1996) 3741.

[18] CTEQ4: H.-L. Lai et al., Phys. Rev. D55 (1997) 1280, http://cteq.org.

[19] S. Dawson. Nucl.Phys. B249 (1985) 42-60.

[20] G.L.Kane, W.W.Repko and W.B.Rolnick, Phys. Lett., 148B (1984) 367.

[21] P.W.Johnson, F.J.Olness, and W.K.Tung, Phys. Rev. D36 (1987).

[22] B.Mele, in *Proceedings of the Workshop on Physics at Future Accelerators*, vol. II, p.13, J. Mulvey, ed. (1987).

[23] M. S. Chanowitz and M. K. Gaillard, Nucl. Phys. B261:379 (1985); H. Veltman Phys. Rev. D41 2294 (1990)

[24] J.Lindfors, Z. Phys. C28 (1985) 427; R.Kauffman, Ph. D. Thesis, SLAC-0348 (1989).

[25] G.P.Lepage, Journal of Computational Physics 27 (1978) 192.

[26] M. Jezabek and J. H. Kühn, Phys. Lett. B329, 317 (1994).